TXNDC9 knockdown inhibits lung adenocarcinoma progression by targeting YWHAG

JING WANG[1], XIAOTAO PAN[2], JIE LI[3] and JIN ZHAO[3]

[1]Respiratory and Critical Care Medicine Department, The Second People's Hospital of Shaanxi Province, Xi'an, Shaanxi 710005; [2]General Surgery Department, Shaanxi Provincial Cancer Hospital, Xi'an, Shaanxi 710600; [3]Radiotherapy Department, Shaanxi Provincial Cancer Hospital, Xi'an, Shaanxi 710600, P.R. China

Received August 20, 2021; Accepted November 17, 2021

DOI: 10.3892/mmr.2022.12719

Abstract. Lung adenocarcinoma (LUAD) is the most common form of lung cancer and with the highest mortality rate. Therefore, the identification and development of effective methods for the treatment of LUAD is of great importance. The present study aimed to investigate the role of thioredoxin domain-containing protein 9 (TXNDC9) and tyrosine 3-monooxygenase/tryptophan 5-monooxygenase activation protein γ (YWHAG; also known as 14-3-3γ) in the progression of LUAD. The expression of TXNDC9 and its association with the survival of patients with LUAD was analyzed using Encyclopedia of RNA Interactomes. Reverse transcription-quantitative PCR and western blot analysis were used to detect TXNDC9 mRNA and protein expression levels, respectively, in *in vitro* studies. To investigate the role of TXNDC9 in the progression of LUAD, TXNDC9 was silenced using small interfering RNA transfection. Furthermore, the viability, proliferation, migration, invasiveness and apoptosis of TXNDC9-silenced A549 cells were detected using Cell Counting Kit (CCK)-8, colony formation, wound healing, Transwell and TUNEL assays, respectively. The association between TXNDC9 and YWHAG was analyzed using STRING and Gene Expression Profiling Interactive Analysis databases, as well as co-immunoprecipitation assays. Subsequently, YWHAG was overexpressed to similarly determine effects of YWHAG on viability, proliferation, migration, invasiveness and apoptosis of A549 cells. TXNDC9 expression was markedly upregulated in lung cancer cells, particularly A549 cells, and silencing of TXNDC9 expression suppressed the viability of the lung cancer cells. The results also revealed that TXNDC9 silencing exerted inhibitory effects on the viability, proliferation, migration and invasiveness of A549 cells, whereas the apoptotic rate was increased. Similar to TXNDC9, YWHAG expression was also upregulated in the A549 cells. Furthermore, TXNDC9 was demonstrated to bind to YWHAG and was positively associated with YWHAG. YWHAG overexpression reversed the inhibitory effects of TXNDC9 silencing on LUAD, as evidenced by increased viability, proliferation, migration and invasiveness, and decreased apoptosis, of A549 cells. The present study demonstrated that the knockdown of TXNDC9 exerted suppressive effects on LUAD, whereas YWHAG overexpression reversed the inhibitory effects of TXNDC9 silencing on LUAD. Therefore, TXNDC9 silencing may exert protective effects against LUAD by targeting YWHAG.

Correspondence to: Professor Jin Zhao, Radiotherapy Department, Shaanxi Provincial Cancer Hospital, 309 Yanta Xi Lu, Xi'an, Shaanxi 710600, P.R. China
E-mail: zjzhaojinzj@163.com

Key words: thioredoxin domain-containing protein 9, tyrosine 3-monooxygenase/tryptophan 5-monooxygenase activation protein γ, 14-3-3γ, lung adenocarcinoma

Introduction

Cancer statistics released in 2018 revealed that lung cancer is the most frequently diagnosed type of cancer, as well as a primary cause of cancer-associated mortality worldwide (1). Non-small cell lung cancer (NSCLC), the most common type of lung cancer, comprises lung squamous cell carcinoma and lung adenocarcinoma (LUAD) (2,3). As a major subtype of lung cancer, LUAD accounts for >40% of lung cancer cases (4). Although progress has been made in diagnostic and treatment methods in recent years, the average 5-year survival rate of patients with lung cancer is ~18% (5). Therefore, elucidation of the underlying mechanisms of LUAD and the identification of more effective therapeutic strategies is of utmost urgency.

Thioredoxin domain-containing protein 9 (TXNDC9; also known as ATP-binding protein associated with cell differentiation or phosducin-like family of proteins 3), belongs to the small, highly-conserved and ubiquitous TRX family which is implicated in multiple biological processes via modulating oxidative stress response (6,7). TXNDC9 is upregulated in numerous types of cancer, promoting their development. For example, Feng *et al* (8) reported that TXNDC9 exerts promotive effects on cell survival and proliferation of prostate cancer. A previous study reported that TXNDC9 is upregulated in colorectal cancer (CRC) and functions as a tumor promoter owing to its promotive role in cell proliferation and invasiveness (9). Moreover, TXNDC9 accelerates hepatocellular carcinoma (HCC) cell proliferation, and TXNDC9

overexpression is associated with poor prognosis of patients with HCC (10). According to results from The Encyclopedia of RNA Interactomes (ENCORI; https://starbase.sysu.edu.cn/panCancer.php), TXNDC9 expression is increased in LUAD and its high expression is associated with poor prognosis (Fig. 1A and B); therefore, it was hypothesized that TXNDC9 may regulate the development of LUAD.

Tyrosine 3-monooxygenase/tryptophan 5-monooxygenase activation protein γ (YWHAG; also known as 14-3-3γ) is a member of the 14-3-3 protein family, a family of highly conserved proteins that regulate signal transduction by binding to phosphoserine-containing proteins (11,12). YWHAG is upregulated in gastric cancer (GC) tissue, and YWHAG knockdown has been shown to inhibit proliferation, migration and invasion of GC cells, and to promote apoptosis (13). Kim *et al* (14) discovered that overexpression of YWHAG promotes proliferation of breast cancer cells. Moreover, YWHAG knockdown effectively inhibits proliferation, migration and invasion of NSCLC (15). Results from Gene Expression Profiling Interactive Analysis (GEPIA) suggested that TXNDC9 is positively associated with YWHAG in LUAD; therefore, it was hypothesized that TXNDC9 may inhibit LUAD progression by targeting YWHAG.

The present study intended to clarify the effects of TXNDC9 on the aggressive properties of LUAD cells and to investigate the underlying mechanism.

Materials and methods

Cell culture, treatment and transfection. Human type II alveolar epithelial cells (BEAS-2B; BCRC 60074) and lung cancer cell lines (H1975, HCC827 and A549) were purchased from the Food Industry Research and Development Institute (Hsinchu, Taiwan). The cells were cultured in DMEM (Gibco; Thermo Fisher Scientific, Inc.) containing 10% FBS (Gibco; Thermo Fisher Scientific, Inc.), 100 U/ml penicillin and 100 μg/ml streptomycin (Invitrogen; Thermo Fisher Scientific, Inc.) at 37˚C in a humidified atmosphere with 5% CO_2. All cell lines used were verified by STR through Applied Biosystems (Thermo Fisher Scientific, Inc.).

For transfection, 20 μM small interfering (si)RNA-negative control (NC; 5'-CACUGAUUUCAAAUGGUGCUAUU-3'), overexpression (Oe) plasmid-NC, si-TXNDC9 (5'-TTTGGTAGTCTGAAGCAGC-3') and Oe-YWHAG were obtained from Shanghai GenePharma Co., Ltd. Cells were incubated with 5% CO_2 at 37˚C and were used in subsequent experiments after 48 h of transfection. Cell transfection was performed using Lipofectamine 2000® Transfection Reagent (Invitrogen; Thermo Fisher Scientific, Inc.) according to the manufacturer's instructions.

Western blot analysis. Total protein extraction from A549 cells was performed using RIPA lysis buffer (Beijing Solarbio Science & Technology Co., Ltd.) and the protein concentrations were quantified using a BCA kit (Beyotime Institute of Biotechnology). Proteins (40 μg/lane) were separated by 12% SDS-PAGE and then transferred onto PVDF membranes. After blocking with 5% non-fat milk for 2 h at room temperature, the membranes were incubated overnight at 4˚C with the following primary antibodies (all purchased from Abcam): Anti-TXNDC9 (1:5,000; cat. no. ab185959), anti-YWHAG (1:1,000; cat. no. ab237732), anti-matrix metalloproteinase (MMP)2 (1:1,000; cat. no. ab92536), anti-MMP9 (1:1,000; cat. no. ab76003), anti-BCL-2 associated X (Bax; 1:1,000; cat. no. ab32503), anti-B-cell lymphoma-2 (Bcl-2; 1:1,000; cat. no. ab32124) and anti-GAPDH (1:2,500; cat. no. ab9485). Following primary incubation, membranes were incubated with goat anti-rabbit horseradish peroxidase-conjugated IgG secondary antibody (1:5,000; cat. no. ab6721; Abcam) at room temperature for 2 h. Protein bands were visualized using enhanced chemiluminescence reagent (cat no. P0018AS; Beyotime Institute of Biotechnology) and protein expression levels were detected and semi-quantified using ImageJ software (version 1.46; National Institutes of Health) with GAPDH as the loading control.

Reverse transcription-quantitative PCR (RT-qPCR). Total RNA from was isolated from the BEAS-2B and A549 cells using TRIzol® reagent and reverse transcribed into cDNA using a SuperScript™ Double-Stranded cDNA Synthesis kit (both Invitrogen; Thermo Fisher Scientific, Inc.). qPCR for gene quantification was performed using SYBR Premix Ex Taq (Takara Bio, Inc.) and an ABI 7500 Fast Real-Time PCR System (Applied Biosystems; Thermo Fisher Scientific, Inc.) according to the manufacturer's protocol. The following thermocycling conditions were used for qPCR: 95˚C for 10 min; followed by 40 cycles of 95˚C for 10 sec and 60˚C for 60 sec. The following primers (purchased from GenScript) were used for qPCR: TXNDC9 forward, 5'-GTGAAAATGTGGTTTGCCATT-3' and reverse, 5'-TGCTTTTTCCACATTCAGCTT-3'; YWHAG forward, 5'-GGAGGGTCATCAGTAGCATTG-3' and reverse, 5'-AGTTATCCAGCAGGCTCAGC-3' and GAPDH forward, 5'-AGCCACATCGCTCAGACAC-3' and reverse, 5'-GCCCAATACGACCAAATCC-3'. GAPDH served as the endogenous control and the calculation of relative gene expression was determined using $2^{-\Delta\Delta Cq}$ method (16).

Cell Counting Kit-8 (CCK-8) assay. A549 cells ($1x10^3$ cells/well) were inoculated into 96-well plates and incubated at 37˚C for 24, 48 and 72 h. Each well was then supplemented with 10 μl CCK-8 reagent (Beyotime Institute of Biotechnology) and incubated for a further 2 h. The absorbance of each well was detected at a wavelength of 50 nm, using a microplate reader (Bio-Rad Laboratories, Inc.).

Colony formation assay. A549 cells were resuspended in DMEM supplemented with 10% FBS for colony formation assay; $5x10^2$ cells/well were seeded in 6-well plates and incubated at 37˚C with 5% CO_2 for 14 days. Subsequently, cells were fixated using 4% paraformaldehyde for 15 min at 37˚C and stained with 0.5% crystal violet solution for 30 min at room temperature. Finally, colonies (>50 cells) were counted manually using an inverted fluorescent microscope (Nikon Corporation; magnification, x100).

Wound healing assay. A549 cells ($1x10^5$ cells/well) were inoculated in 6-well plates and incubated at 37˚C until the cell confluency reached 90-100%. A linear scratch in the cell monolayer was then made using a pipette tip. The cells were washed three times with PBS to remove cellular debris and

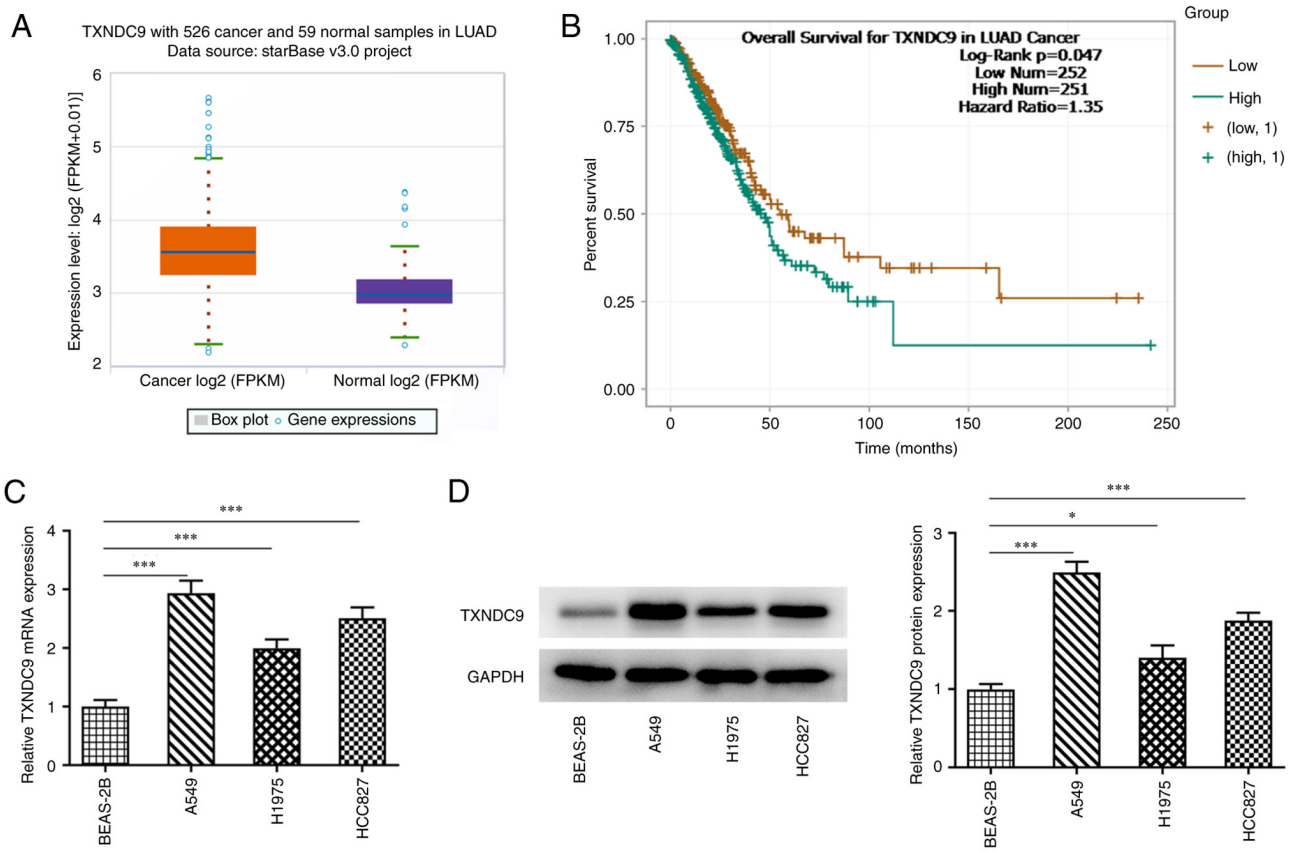

Figure 1. TXNDC9 is upregulated in LUAD cells. (A) Encyclopedia of RNA Interactomes revealed that TXNDC9 was upregulated in LUAD. (B) Overall survival for high TXNDC9 expression and low TXNDC9 expression in LUAD cancer; + (low,1) represents one sample in low TXNDC9 expression group, + (high,1) represents one sample in high TXNDC9 expression group. Relative TXNDC9 (C) mRNA and (D) protein expression levels were measured using reverse transcription-quantitative PCR and western blotting, respectively. *P<0.05 and ***P<0.001. LUAD, lung adenocarcinoma; TXNDC9, thioredoxin domain-containing protein 9.

incubated at 37˚C and 5% CO_2. Images were captured by a light microscope at 0 and 24 h, and the area of migrated cells in the linear scratch).

TUNEL assay. The effect of TXNDC9 silencing on A549 cell apoptosis was detected using TUNEL detection solution (Beyotime Institute of Biotechnology) according to the manufacturer's protocol. In brief, A549 cells (1x10^6 cells/well) were fixed with 4% paraformaldehyde for 15 min at room temperature and permeabilized in 0.25% Triton X-100 for 20 min at room temperature. Subsequently, after cells were rinsed with PBS, TdT solution and dUTP solution were added and incubated at 37˚C for 1 h in the dark. Cells were treated with 10 μg/ml DAPI for nucleus staining for 5 min at 37˚C and mounted in an anti-fade reagent (Beijing Solarbio Science & Technology Co., Ltd.). In total, three fields of view were selected at random and an inverted fluorescence microscope (magnification, x100; Olympus Corporation) was used to observe the excitation and emission wavelengths at 450-500 and 515-565 nm, respectively.

Co-immunoprecipitation (co-IP) assay. STRING (string-db.org) and GEPIA (gepia.cancer-pku.cn) databases revealed that TXNDC9 was positively associated with YWHAG and bound to YWHAG. To verify this, co-IP assays were performed. Total proteins from the A549 cells were isolated using RIPA lysis buffer (Beijing Solarbio Science & Technology Co., Ltd.) and quantified using BCA kit (Beyotime Institute of Biotechnology). For immunoprecipitation, 500 μg protein was incubated with 2 μg appropriate antibodies including TXNDC9 (1:50; cat. no. ab185959; Abcam), YWHAG (1:200; cat. no. ab237732; Abcam) and IgG (1:2,000; cat. no. A0208; Beyotime Institute of Biotechnology) overnight at 4˚C. Subsequently, 40 μl Protein G/A agarose beads (Invitrogen; Thermo Fisher Scientific, Inc.) were added to cell lysate and incubated for 2 h. After beads were washed with PBS three times, precipitated proteins were re-suspended in 2X SDS-PAGE loading buffer, boiled for 5 min and eluted from the beads. Finally, western blot analysis was used to measure the products from IP as aforementioned.

Bioinformatics tools. ENCORI database (https://starbase.sysu.edu.cn/panCancer.php) was used to detect TNXDC9 expression in LUAD and to analyze the association between TNXDC9 and the overall survival rate of LUAD patients. GEPIA database (http://gepia.cancer-pku.cn/) was used to explore the correlation between TNXDC9 and YWHAG in LUAD.

Statistical analysis. Data are presented as the mean ± SD. All experiments were performed in triplicate. Statistical analysis

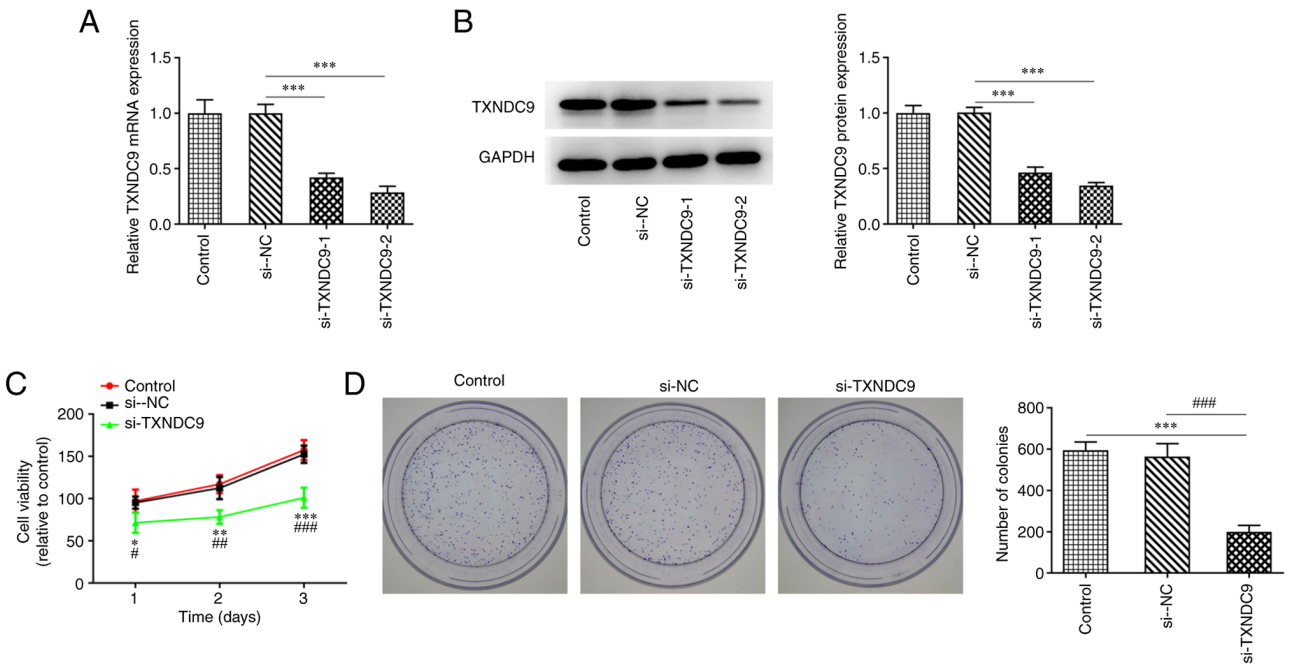

Figure 2. TXNDC9 knockdown inhibits viability and proliferation of lung adenocarcinoma cells. Relative (A) mRNA and (B) protein expression levels of TXNDC9 were measured using reverse transcription-quantitative PCR and western blot, respectively. ***P<0.001. (C) Cell viability was detected using Cell Counting Kit-8. $^{\#}$P<0.05, $^{\#\#}$P<0.01 and $^{\#\#\#}$P<0.001 vs. si-NC; *P<0.05, **P<0.01 and ***P<0.001 vs. Control. (D) Proliferation was detected using colony formation assay, magnification, x4. ***P<0.001 vs. Control; $^{\#\#\#}$P<0.001 vs. si-NC. NC, negative control; si, small interfering; TXNDC9, thioredoxin domain-containing protein 9.

was performed using SPSS 20.0 software (IBM Corp.). One-way ANOVA was used to perform statistical analysis followed by Tukey's multiple comparisons post hoc test. The survival of LUAD patients was subjected to Kaplan-Meier analysis. Correlation between TNXDC9 and YWHAG was evaluated using Pearson's correlation analysis. P<0.05 was considered to indicate a statistically significant difference.

Results

TXNDC9 is upregulated in LUAD cells. The results from ENCORI suggested that TXNDC9 was markedly upregulated in LUAD cells (Fig. 1A). Additionally, poor survival of patients with LUAD was observed in the high TXNDC9 expression group compared with the low TXNDC9 expression group (Fig. 1B). The relative mRNA and protein expression levels of TXNDC9 in normal lung epithelial (BEAS-2B0 and lung cancer cells (A549, H1975 and HCC827 cells) were detected using RT-qPCR and western blot analysis. Compared with BEAS-2B normal epithelial cells, relative TXNDC9 mRNA and protein expression in lung cancer cells was significantly upregulated, particularly in A549 cells (Fig. 1C and D, respectively). Therefore, A549 cells were selected for use in subsequent experiments.

TXNDC9 knockdown inhibits viability and proliferation of LUAD cells. To investigate the effects of TXNDC9 on LUAD cells, A549 cells were transfected with si-TXNDC9-1/2. mRNA and protein expression levels of TXNDC9 were significantly decreased in the TXNDC9-silenced A549 cells compared with the si-NC group (Fig. 2A and B). si-TXNDC9-2 was chosen for the subsequent experiments as it displayed an improved interference efficiency compared with si-TXNDC9-1. In addition, CCK-8 and colony formation assay results demonstrated that the viability and the proliferation, respectively, of A549 cells were significantly diminished by TXNDC9 silencing compared with the controls (Fig. 2C and D), revealing that TXNDC9 knockdown exerted inhibitory effects on the proliferation of LUAD cells.

TXNDC9 knockdown inhibits migration and invasion, and promotes apoptosis, of LUAD cells. Wound healing and Transwell assays were used to determine the relative migration rate and invasive ability. TXNDC9 silencing significantly suppressed the migration rate of A549 cells compared with the si-NC group (Fig. 3A and B); TXNDC9 silencing similarly inhibited A549 cell invasiveness (Fig. 3C and D). Additionally, the effects of TXNDC9 knockdown on apoptosis of A549 cells was detected using TUNEL assay. TXNDC9 knockdown significantly promoted apoptosis of A549 cells (Fig. 3E and F). Moreover, the protein expression levels of matrix metalloproteinase (MMP)2, MMP9 and Bcl-2 were significantly decreased by TXNDC9 knockdown, whereas relative Bax protein expression was significantly increased (Fig. 3G).

YWHAG is upregulated in LUAD and binds to TXNDC9. The mRNA and protein expression levels of YWHAG were higher in A549 LUAD cells compared with BEAS-2B normal lung epithelial cells (Fig. 4A and B). According to STRING and GEIPA databases, YWHAG and TXNDC9 were co-expressed and positively correlated with each other (Fig. 4C and D). Considering the positive association between YWHAG and TXNDC9, co-IP assay was performed to verify the binding between YWHAG and TXNDC9. TXNDC9 was observed with anti-YWHAG and YWHAG was observed

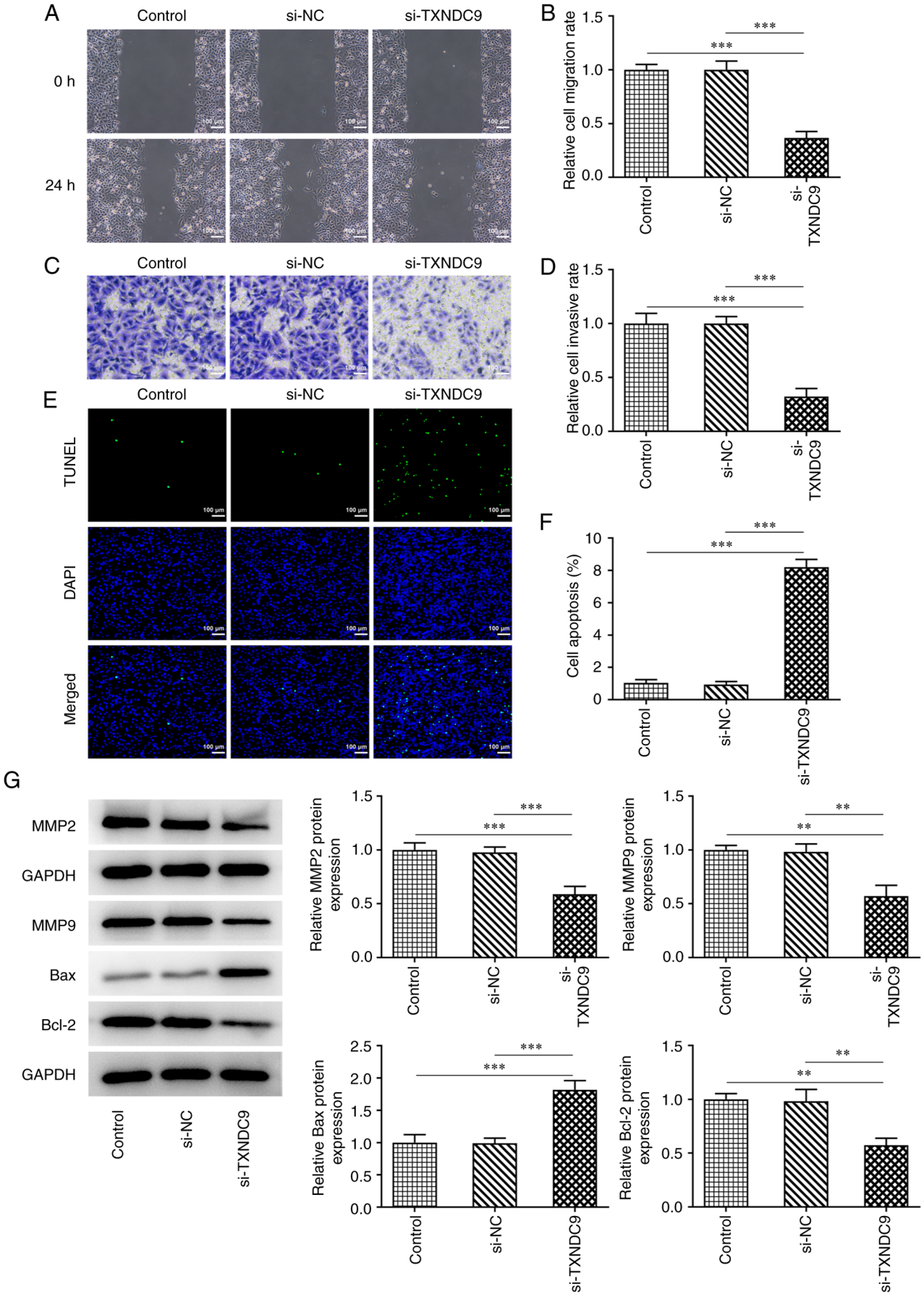

Figure 3. TXNDC9 knockdown inhibits migration and invasion, and promotes apoptosis, of lung adenocarcinoma cells. (A) Wound healing and (B) quantitative analysis. (C) Transwell and (D) relative invasion rate. (E) TUNEL assay and (F) quantitative analysis. (G) Protein expression levels of MMP2, MMP9, Bax and Bcl-2 were detected using western blotting. **P<0.01, ***P<0.001. MMP, matrix metalloproteinase; NC, negative control; si, small interfering RNA; TXNDC9, thioredoxin domain-containing protein 9.

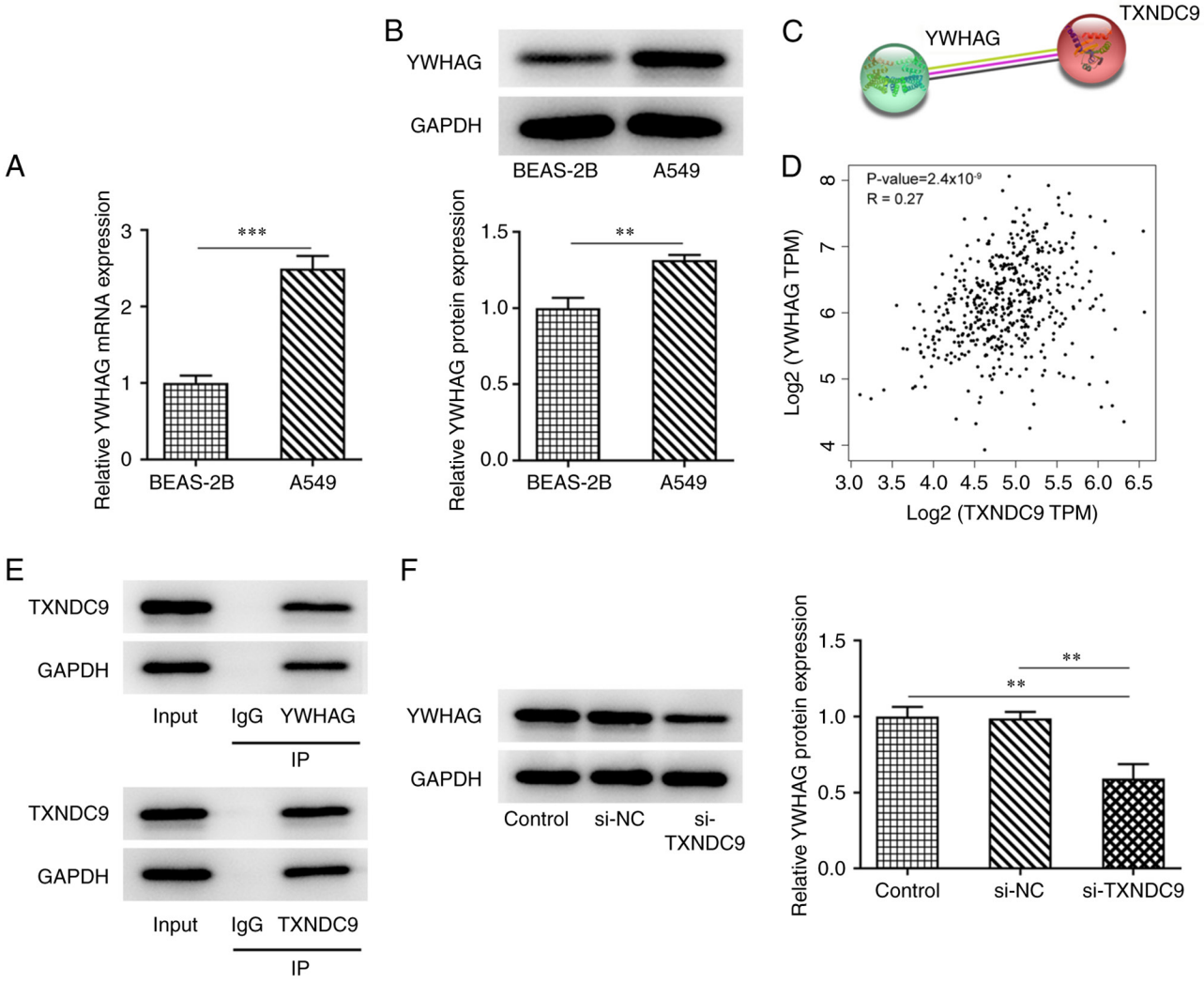

Figure 4. YWHAG is upregulated in lung adenocarcinoma and binds to TXNDC9. (A) mRNA and (B) protein expression levels of YWHAG were measured using reverse transcription-quantitative PCR and western blot, respectively. (C) According to STRING database, TXNDC9 and YWHAG are co-expressed and (D) Gene Expression Profiling Interactive Analysis revealed that TXNDC9 was positively correlated with YWHAG. (E) TXNDC9 and YWHAG were detected using co-IP. (F) Protein expression of YWHAG was measured using western blotting following si-TXNDC9 transfection. **P<0.01, ***P<0.001. IP, immunoprecipitation; si, small interfering; NC, negative control; TPM, transcripts per million; TXNDC9, thioredoxin domain-containing protein 9; YWHAG, tyrosine 3-monooxygenase/tryptophan 5-monooxygenase activation protein γ.

with anti-TXNDC9, revealing that TXNDC9 bound to YWHAG (Fig. 4E). Compared with the si-NC group, the expression of YWHAG was decreased in TXNDC9-silenced A549 cells (Fig. 4F).

YWHAG overexpression reverses the inhibitory effect of TXNDC9 silencing on viability, proliferation, migration and invasion of LUAD cells. A549 cells were transfected with Oe-YWHAG, and the relative mRNA and protein expression of YWHAG were significantly upregulated compared with the Oe-NC-transfected group (Fig. 5A and B). Decreased cell viability and proliferation induced by TXNDC9 knockdown were partially reversed by YWHAG overexpression (Fig. 5C-E), suggesting that overexpression of YWHAG decreased the inhibitory effects of TXNDC9 silencing on A549 cell viability and proliferation. Furthermore, compared with the si-TXNDC9 + Oe-NC group, the decrease in migratory (Fig. 5F and G) and invasive rates (Fig. 5H and I) of the A549 cells were partially reversed following transfection with YWHAG overexpression vector.

YWHAG overexpression reverses the promotive effects of TXNDC9 silencing on LUAD cell apoptosis. TUNEL assay was used to detect the effects of YWHAG overexpression on the apoptosis of TXNDC9-silenced A549 cells. The results demonstrated that the increased apoptosis observed following TXNDC9 silencing was decreased by overexpression of YWHAG compared with the si-TXNDC9 + Oe-NC group (Fig. 6A and B), which indicated that YWHAG overexpression diminished the promotive effects of TXNDC9 on cell apoptosis. Furthermore, the protein levels of apoptosis-related factors including Bax and Bcl-2 and metastasis-related factors including MMP2 and MMP9 were tested. It was found that the downregulated expression levels of MMP2, MMP9 and Bcl-2 were upregulated by YWHAG overexpression, whereas upregulated Bax expression was downregulated (Fig. 6C).

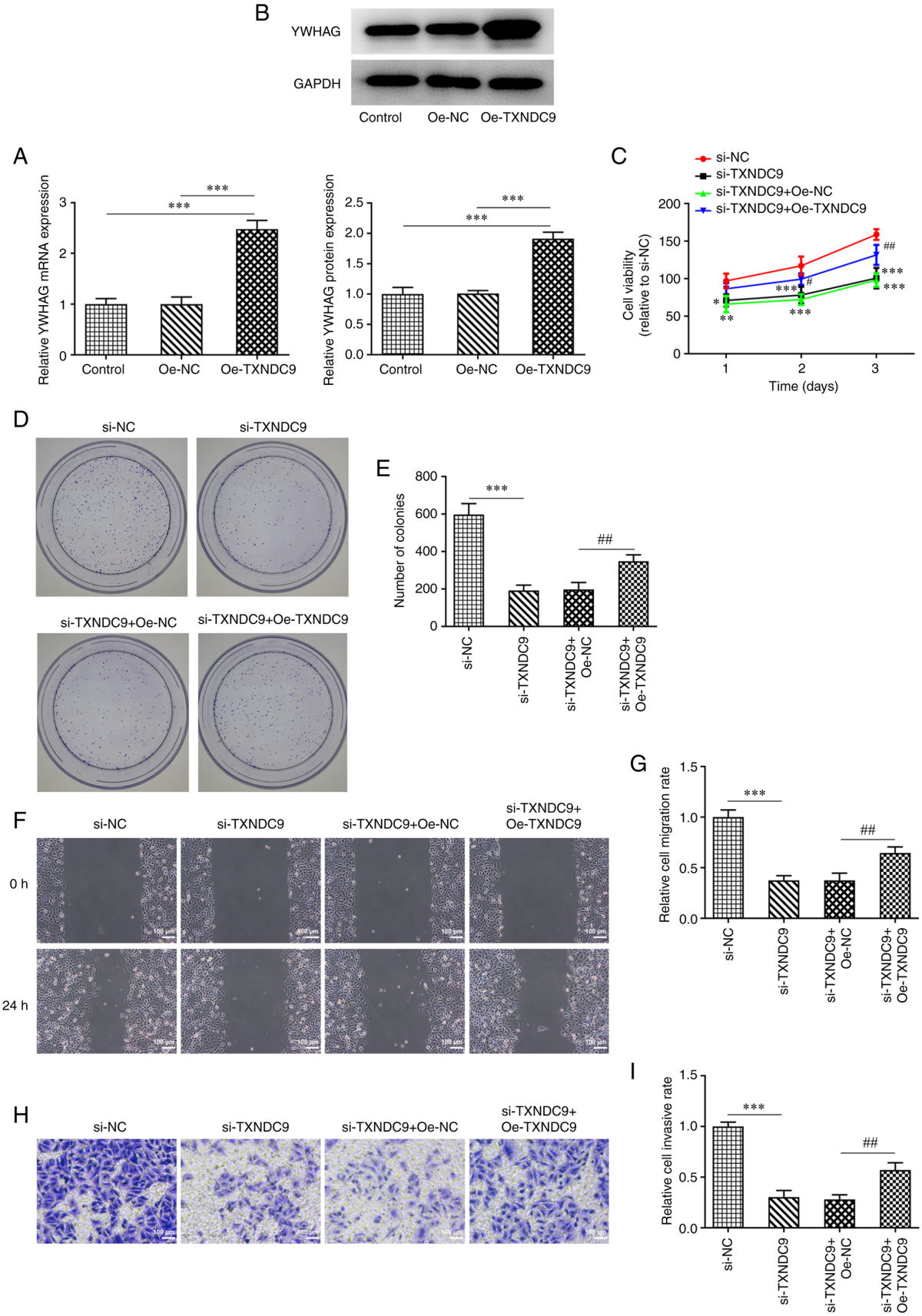

Figure 5. YWHAG overexpression reverses the inhibitory effect of TXNDC9 silencing on the viability, proliferation, migration and invasiveness of lung adenocarcinoma cells. (A) mRNA and (B) protein expression levels of YWHAG were measured using reverse transcription-quantitative PCR and western blotting, respectively. ***P<0.001 vs. Oe-NC or Control. (C) Cell viability was detected using Cell Counting Kit-8 assay. *P<0.05, **P<0.01, ***P<0.001 vs. si-NC; $^{\#}$P<0.05 and $^{\#\#}$P<0.01 vs. si-TXNDC9 + Oe-NC. (D and E) Proliferation was detected using colony formation assay. Magnification, x4. ***P<0.001 vs. si-NC; $^{\#\#}$P<0.01 vs. si-TXNDC9 + Oe-NC. (F and G) Wound healing and (H and I) Transwell assay were used to detect migration and invasiveness, respectively. ***P<0.001 vs. si-NC; $^{\#\#}$P<0.01 vs. si-TXNDC9 + Oe-NC. NC, negative control; Oe, overexpression; si, small interfering RNA; TXNDC9, thioredoxin domain-containing protein 9; YWHAG, tyrosine 3-monooxygenase/tryptophan 5-monooxygenase activation protein γ.

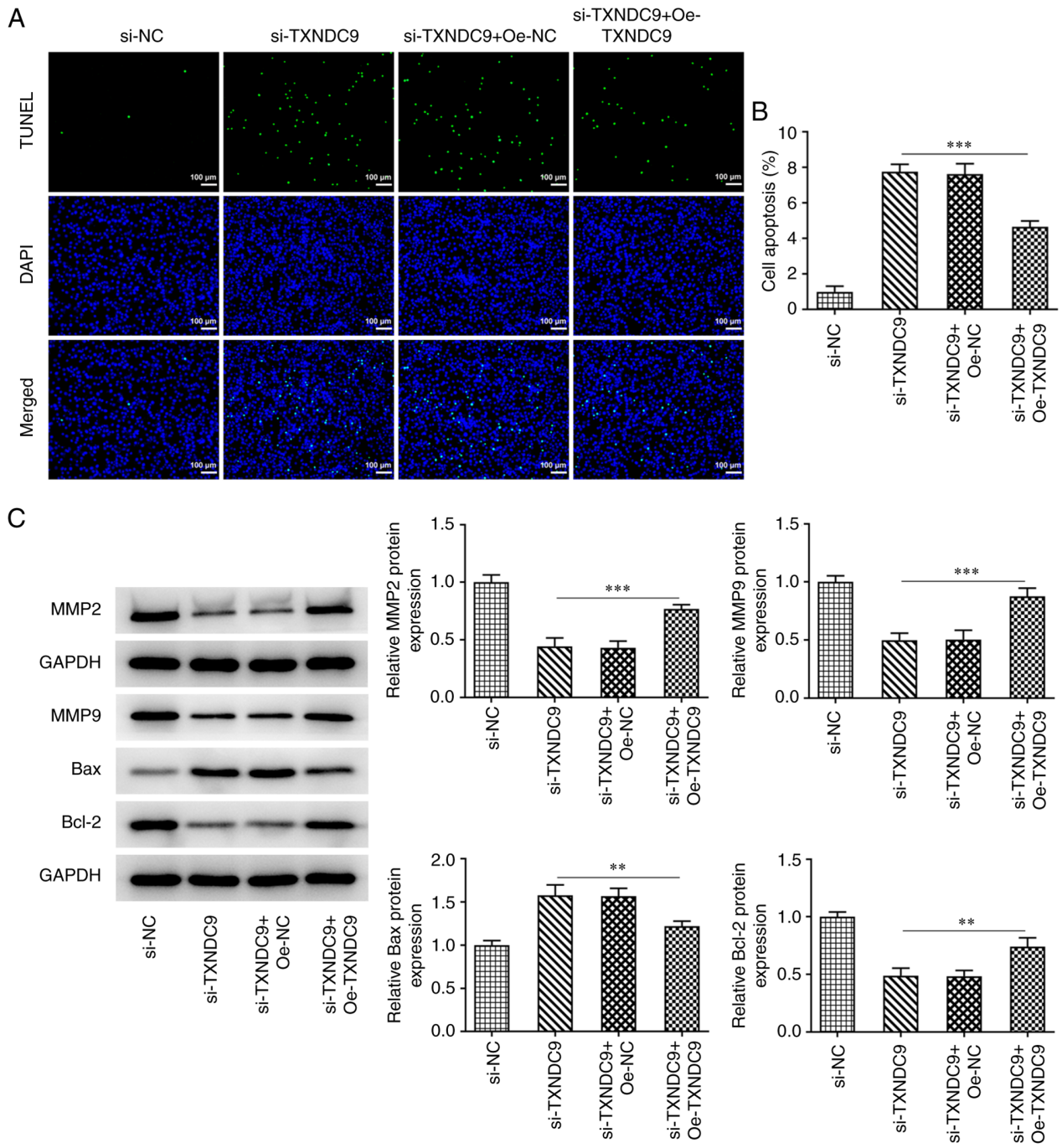

Figure 6. YWHAG overexpression reverses the promotive effects of TXNDC9 silencing on lung adenocarcinoma cells apoptosis. (A) Representative images and (B) quantitative analysis of the TUNEL assay used to examine apoptosis. (C) Protein expression levels of MMP2, MMP9, Bax and Bcl-2 were detected using western blot analysis. **P<0.01, ***P<0.001. MMP, matrix metalloproteinase; NC, negative control; oe, overexpression; si, small interfering; TXNDC9, thioredoxin domain-containing protein 9; YWHAG, tyrosine 3-monooxygenase/tryptophan 5-monooxygenase activation protein γ.

Discussion

Lung cancer poses a serious threat to human health and is one of the most aggressive and lethal types of cancer worldwide (17). The recorded lung cancer mortality rate increased by 464.84% in the past 30 years in China (18). To date, effective methods for treatment of LUAD are lacking (19). It is well documented that TRX system protects against oxidative stress and inflammation in lung diseases (20). In addition, serum thioredoxin level has been discovered to be elevated in on-small cell lung carcinoma patients (21).

Several studies have revealed that TXNDC9 has an abnormal expression in various types of cancer (22,23). A previous study reported that TXNDC9 expression is upregulated a serves a key role in CRC (22). Expression of TXNDC9 is also increased in breast cancer cells (24). Moreover, Chen *et al* (10) observed that TXNDC9 promotes HCC progression, whereas TXNDC9 knockdown inhibits proliferation of HCC cells. Consistent with these findings, in the present study, TXNDC9 expression was demonstrated to be upregulated in lung cancer cells compared with normal lung epithelial. Moreover, TXNDC9 knockdown inhibited the

viability and proliferation of A549 cells in LUAD. Silencing of TXNDC9 abrogated cell migration and invasion in LUAD, accompanied by downregulated MMP2 and MMP9 protein levels. By contrast, TXNDC9 knockdown promoted the apoptosis of A549 cells by increasing Bax expression and decreasing Bcl-2 expression. These results suggested that TXNDC9 knockdown inhibited LUAD progression, which implied that TXNDC9 might primarily serve as an oncogene in multiple malignancies, LUAD included.

YWHAG has been reported to be involved in various biological processes, particularly in cancer (25). For example, an effective treatment for skin cancer is targeting of the interaction of YWHAG with CDC25A (26). YWHAG has been shown to promote cell motility in breast cancer and inhibition of YWHAG may serve as a novel therapeutic target for the treatment of breast cancer (27). Qi *et al* (28) demonstrated that YWHAG serves a key role in regulating cell cycle progression and its overexpression contributes to polyploidization in H322 lung cancer cells. In the present study, the expression of YWHAG was upregulated in lung cancer cells, which is consistent with a previous study (15). The elevated expression of YWHAG in certain types of human cancer suggests that YWHAG may function as an oncogene (29). Therefore, YWHAG may represent an effective therapeutic target for the treatment of lung cancer.

According to STRING and GEIPA, TXNDC9 was co-expressed and was positively correlated with YWHAG; therefore, further experiments were performed to confirm this prediction. Considering that TXNDC9 was involved in LUAD progression, it was hypothesized that TXNDC9 may target YWHAG to inhibit the viability, proliferation, migration and invasiveness of lung cancer cells and promote apoptosis, thus exerting inhibitory effects on LUAD progression. YWHAG overexpression abolished the inhibitory effects of TXNDC9 silencing on A549 cells. However, the present study only conducted *in vitro* experiments, and *in vivo* experiments in mice need to be performed. It is also important to verify the interaction between TXNDC9 and YWHAG for screening other lung cancer cell lines. Furthermore, the present study only investigated the effect of TXNDC9 and YWHAG interaction on LUAD; other mechanisms downstream of YWHAG need to be explored in the future.

In conclusion, the present study demonstrated that TXNDC9 and YWHAG were upregulated in LUAD, and that TXNDC9 bound to YWHAG. TXNDC9 knockdown inhibited LUAD progression, and YWHAG overexpression reversed these inhibitory effects.

Acknowledgements

Not applicable.

Funding

No funding was received.

Availability of data and materials

The datasets used and/or analyzed during the current study are available from the corresponding author on reasonable request.

Authors' contributions

JW and XP conceived and designed the study. JL and JZ performed the experiments. XP and JL analyzed the experimental data. JW and JZ wrote and revised the manuscript. XP and JL confirm the authenticity of all the raw data. All authors have read and approved the final manuscript.

Ethics approval and consent to participate

Not applicable.

Patient consent for publication

Not applicable.

Competing interests

The authors declare that they have no competing interests.

References

1. Bray F, Ferlay J, Soerjomataram I, Siegel RL, Torre LA and Jemal A: Global cancer statistics 2018: GLOBOCAN estimates of incidence and mortality worldwide for 36 cancers in 185 countries. CA Cancer J Clin 68: 394-424, 2018.
2. Gridelli C, Rossi A, Carbone DP, Guarize J, Karachaliou N, Mok T, Petrella F, Spaggiari L and Rosell R: Non-small-cell lung cancer. Nat Rev Dis Primers 1: 15009, 2015.
3. Song Q, Shang J, Yang Z, Zhang L, Zhang C, Chen J and Wu X: Identification of an immune signature predicting prognosis risk of patients in lung adenocarcinoma. J Transl Med 17: 70, 2019.
4. Travis WD: Lung cancer pathology: Current concepts. Clin Chest Med 41: 67-85, 2020.
5. Siegel RL, Miller KD and Jemal A: Cancer statistics, 2018. CA Cancer J Clin 68: 7-30, 2018.
6. Ma F, Hou L and Yang L: Txndc9 is required for meiotic maturation of mouse oocytes. Biomed Res Int 2017: 6265890, 2017.
7. Kang CH, Park JH, Lee ES, Paeng SK, Chae HB, Hong JC and Lee SY: Redox-dependent structural modification of nucleoredoxin triggers defense responses against alternaria brassicicola in arabidopsis. Int J Mol Sci 21: 9196, 2020.
8. Feng T, Zhao R, Sun F, Lu Q, Wang X, Hu J, Wang S, Gao L, Zhou Q, Xiong X, *et al*: TXNDC9 regulates oxidative stress-induced androgen receptor signaling to promote prostate cancer progression. Oncogene 39: 356-367, 2020.
9. Lu A, Wangpu X, Han D, Feng H, Zhao J, Ma J, Qu S, Chen X, Liu B and Zheng M: TXNDC9 expression in colorectal cancer cells and its influence on colorectal cancer prognosis. Cancer Invest 30: 721-726, 2012.
10. Chen D, Zou J, Zhao Z, Tang X, Deng Z, Jia J and Liu S: TXNDC9 promotes hepatocellular carcinoma progression by positive regulation of MYC-mediated transcriptional network. Cell Death Dis 9: 1110, 2018.
11. Aitken A: 14-3-3 proteins: A historic overview. Semin Cancer Biol 16: 162-172, 2006.
12. Cho E and Park JY: Emerging roles of 14-3-3γ in the brain disorder. BMB Rep. BMB Rep 53: 500-511, 2020.
13. Ni J, Wang J, Fu Y, Yan C, Zhu M, Jiang Y, Chen J, Ding Y, Fan X, Li G and Jin G: Functional genetic variants in centrosome-related genes CEP72 and YWHAG confer susceptibility to gastric cancer. Arch Toxicol 94: 2861-2872, 2020.
14. Kim JO, Kim SR, Lim KH, Kim JH, Ajjappala B, Lee HJ, Choi JI and Baek KH: Deubiquitinating enzyme USP37 regulating oncogenic function of 14-3-3γ. Oncotarget 6: 36551-36576, 2015.
15. Wang P, Deng Y and Fu X: MiR-509-5p suppresses the proliferation, migration, and invasion of non-small cell lung cancer by targeting YWHAG. Biochem Biophys Res Commun 482: 935-941, 2017.
16. Livak KJ and Schmittgen TD: Analysis of relative gene expression data using real-time quantitative PCR and the 2(-Delta Delta C(T)) method. Methods 25: 402-408, 2001.

17. Denisenko TV, Budkevich IN and Zhivotovsky B: Cell death-based treatment of lung adenocarcinoma. Cell Death Dis 9: 117, 2018.
18. She J, Yang P, Hong Q and Bai C: Lung cancer in China: Challenges and interventions. Chest 143: 1117-1126, 2013.
19. Zhang C, Zhang Z, Zhang G, Zhang Z, Luo Y, Wang F, Wang S, Che Y, Zeng Q, Sun N and He J: Clinical significance and inflammatory landscapes of a novel recurrence-associated immune signature in early-stage lung adenocarcinoma. Cancer Lett 479: 31-41, 2020.
20. Xu J, Li T, Wu H and Xu T: Role of thioredoxin in lung disease. Pulm Pharmacol Ther 25: 154-162, 2012.
21. Fan J, Yu H, Lv Y and Yin L: Diagnostic and prognostic value of serum thioredoxin and DJ-1 in non-small cell lung carcinoma patients. Tumour Biol 37: 1949-1958, 2016.
22. Zhou W, Fang C, Zhang L, Wang Q, Li D and Zhu D: Thioredoxin domain-containing protein 9 (TXNDC9) contributes to oxaliplatin resistance through regulation of autophagy-apoptosis in colorectal adenocarcinoma. Biochem Biophys Res Commun 524: 582-588, 2020.
23. Wu Y, Ye H, Peng B, Jiang H, Tang Q, Liu Y, Xi J and Chen S: MiR-643 functions as a potential tumor suppressor in gastric cancer by inhibiting cell proliferation and invasion via targeting TXNDC9. Ann Clin Lab Sci 51: 494-502, 2021.
24. Garcia SA and Nagai MA: Transcriptional regulation of bidirectional gene pairs by 17-β-estradiol in MCF-7 breast cancer cells. Braz J Med Biol Res 44: 112-122, 2011.
25. Raungrut P, Wongkotsila A, Lirdprapamongkol K, Svasti J, Geater SL, Phukaoloun M, Suwiwat S and Thongsuksai P: Prognostic significance of 14-3-3γ overexpression in advanced non-small cell lung cancer. Asian Pac J Cancer Prev 15: 3513-3518, 2014.
26. Holmes TR, Al-Matouq J, Holmes M, Nicola L, Rudd JC, Lovas S and Hansen LA: Targeting 14-3-3ε-CDC25A interactions to trigger apoptotic cell death in skin cancer. Oncotarget 11: 3267-3278, 2020.
27. Hiraoka E, Mimae T, Ito M, Kadoya T, Miyata Y, Ito A and Okada M: Correction to: Breast cancer cell motility is promoted by 14-3-3γ. Breast Cancer 26: 594, 2019.
28. Qi W, Liu X, Chen W, Li Q and Martinez JD: Overexpression of 14-3-3gamma causes polyploidization in H322 lung cancer cells. Mol Carcinog 46: 847-856, 2007.
29. Qi W, Liu X, Qiao D and Martinez JD: Isoform-specific expression of 14-3-3 proteins in human lung cancer tissues. Int J Cancer 113: 359-363, 2005.